Supplementary Information for 2019-00703P

TMEM16A controls EGF-induced calcium signaling implicated in pancreatic cancer prognosis

David Crottès[1], Yu-Hsiu T. Lin[2], Christian J. Peters[1], John M. Gilchrist[1], Arun P. Wiita[2], Yuh Nung Jan[1] and Lily Yeh Jan[1*]

[1]Departments of Physiology, Biochemistry, and Biophysics, Howard Hughes Medical Institute, University of California, San Francisco, San Francisco, CA 94143, USA

[2]Department of Laboratory Medicine, University of California, San Francisco, San Francisco, CA 94143, USA

* Correspondence: lily.jan@ucsf.edu

This PDF file includes:

Supplementary text
References for SI reference citations
Figs. S1 to S5
Captions for dataset S1 to S4

Other supplementary materials for this manuscript include the following:

Movies S1 to Sx
Datasets S1 to S4

www.pnas.org/cgi/doi/10.1073/pnas.1900703116

Supplementary Text.

Immunofluorescence. Forty-eight hours prior to the experiment, subconfluent cells were trypsinized and plated on the top of 12 mm coverglass 1.0 in a 24-well plate. The day before experiment, media was replaced by a serum-free media and subjected to overnight (16-20h) incubation. On the day of the experiment, cells were stimulated with or without EGF (50 ng/mL) for various time points and fixed with paraformaldehyde (PFA) 4% solution at RT for 15 minutes. Coverslips were rinsed twice with cold PBS, permeabilized with 0,5% Triton X-100 for 5 min at RT, rinsed three times with PBS and then incubated with blocking solution (PBS containing 0,2% BSA, 0,02% Na-Azide , 0,05% Triton X-100 and 10% FBS) for 1 hr at RT. Coverslips were then incubated overnight at 4°C in primary antibody in IF buffer ((PBS, 0,2% BSA, 0,02% Na-Azide, 0,05% Triton X-100). The next day, coverslips were washed 3-5 times in PBS and incubated with secondary antibodies fro 2h at RT. Coverslips were then washed twice in PBS1and nuclei were stained using Hoescht 33342 (1/1000) for 5 min. Coverslips were then washed one more time and were mounted on top of coverglass using VectaShield Mounting medium (Vector Labs, Burlingame, CA, USA). For the staining of extracellular epitope of EGFR, coverslips were incubated with mouse anti-EGFR (extracellular) 1h at RT in PBS prior to the permeabilization step. Images were acquired using Leica SP8 microscope (Leica, Buffalo Grove, IL, USA) and were processed and analyzed using ImageJ/Fiji software (NIH, Bethesda, USA).

Western Blot. Sub-confluent adherent cells are lysed in Lysis buffer 10 mM Tris-HCl pH 7.5; 150 mM NaCl; 0.5 mM EDTA; 0.5% NP-40) supplemented with Complete EDTA-free protease inhibitor and PhosphoSTOP (Millipore Sigma, Saint-Louis, MO, USA). Whole cell lysate are diluted in 4x LDS sample buffer and resolved on a 4-12% NuPAGE gradient gel, transferred to 0.2 µm nitrocellulose membrane using a semi-dry blotter, blocked for 1 hr in 5% milk in TBST (20 mM Tris, 150 mM NaCl, 0.1% Tween-20), and incubated overnight in primary antibody in 1% milk in TBST. Blots were washed 3-5 times in ddH2O and once in TBST on the next day, incubated with HRP-conjugated secondary antibody, washed 3 times in TBST, and developed with ECL and imaged using Li-Cor C-digit scanner (Lincoln, NE, USA). For the staining of phosphorylated proteins, milk was replaced by BSA. A list of antibodies used for western blot is provided in supplemental table.

RT-PCR. Subconfluent AsPC-1 cells were lysed using Trizol, snap frozen on dry ice and stored at -80°C. RNA extraction was performed using phenol/chloroform and isopropyl alcohol method. cDNA were prepared from RNA using Superscript III First-Strand cDNA synthesis (Thermofischer, Waltham, MA, USA) and according to the manufacturer's recommendation. PCR were then performed on these cDNA using GoTaq Green Master Mix and following provider's recommandations (Promega, Madison, WI, USA).

Immunohistochemistry of human tissues samples. Data were obtained from the Human Protein Atlas (using ANO1 as gene reference in the version 18 of human protein atlas: https://v18.proteinatlas.org) (1, 2).

RNA-seq transcriptomic data. RNA-Seq data from pancreatic cancer and normal pancreas were generated by The Cancer Genome Atlas Research Network (http://cancergenome.nih.gov/) (3) and Genotype Tissue Expression consortium respectively (4, 5). The Genotype-Tissue Expression (GTEx) Project was supported by the Common Fund of the Office of the Director of the National Institutes of Health, and by NCI, NHGRI, NHLBI, NIDA, NIMH, and NINDS. Logarithmic transformed normalized

data (including data expressed as TPM units) from TCGA-PAAD dataset and GTEx dataset were obtained from UCSC Xena Browser (https://xena.ucsc.edu) (6). Raw data from TCGA-PAAD dataset were obtained from GDAC FireBrowse (http://firebrowse.org/) (doi:10.7908/C11G0KM9). Survival analysis was performed using “survival” packages from R software.

Differential expression analysis (DEA). Differential expression analysis were obtained using “DESeq2” package from R / Bioconductor software (https://cran.r-project.org/ https://bioconductor.org/) on raw data obtained by GDAC Firehose and generated by TCGA. DEA was obtained by comparing groups defined according to TMEM16A expression (Figure 1) or clusters defined using our gene-set (Figure 6), Logarithmic transformed data generated by DESeq2 packages were used for the generation of heatmap using “pheatmap” package.

Microarray-based transcriptomic data. Published transcriptomic data of normal and pancreatic cancer generated by microarrays (7–16) were collected on NCBI GEO database (https://www.ncbi.nlm.nih.gov/geo/) (Barrett et al., 2013). For each selected series, raw data were downloaded and RMA pre-processed using “affy” package in R / Bioconductor software.

Gene Set Enrichment Analysis. Gene set enrichment analysis were performed on the $\log_2$(Fold Change)-ranked gene lists obtained by DEA using the GSEA software developed by Broad Institute and gene set collections from the Bader Lab (http://baderlab.org - Human_GOBP_AllPathways_no_GO_iea.October_01_2018_symbol.gmt) (17).

Pathways, string and EnrichmentMap visualization. ErbB pathway visualization was performed using Wikipathway app inside Cytoscape 3.6.1 and by mapping each individual nodes (color, size and font size) with the maximal $\log_2$ fold change observed for each protein obtained by the DEA between “High TMEM16A” and “Low TMEM16A” pancreatic tumors of the TCGA-PAAD dataset. Enrichment of the initial gene set with the addition of ten closest interactors was realized using StringApp inside Cytoscape 3.6.1 (confidence = 0.8) (http://cytoscape.org). Network analysis of data generated by GSEA was performed using EnrichmentMap inside Cytoscape 3.6.1 (Merico et al., 2010) (FDR $p < 0.01$).

PCA and k-means clusterization. From the $\log_2$ transformed data obtained after DESeq2 processing, values for our gene set were isolated and selected. On these values, a Principal Component Analysis was performed using “prcomp” function of the “stat” package from R. k-means clustering was performed using “kmeans” function of the “stat” package from R with the optimal number of clusters k determined using the “NbClust” package (providing the best clustering scheme after compiling 30 different algorithms used for determining the numbers of clusters). Samples were then plot using PCA values and differentiated according to the cluster they belong.

References for SI reference citations

1. Uhlen M, et al. (2017) A pathology atlas of the human cancer transcriptome. *Science* 357(6352). doi:10.1126/science.aan2507.

2. Uhlén M, et al. (2015) Proteomics. Tissue-based map of the human proteome. *Science* 347(6220):1260419.

3. The Cancer Genome Atlas (2017) Integrated Genomic Characterization of Pancreatic Ductal Adenocarcinoma. *Cancer Cell* 32(2):185-203.e13.

4. Carithers LJ, Moore HM (2015) The Genotype-Tissue Expression (GTEx) Project. *Biopreservation Biobanking* 13(5):307–308.

5. Gamazon ER, et al. (2018) Using an atlas of gene regulation across 44 human tissues to inform complex disease- and trait-associated variation. *Nat Genet* 50(7):956–967.

6. Zhu J, et al. (2015) Abstract B1-07: Using the UCSC Xena Platform to integrate, visualize, and analyze your own data in the context of large external genomic datasets. *Cancer Res* 75(22 Supplement 2):B1-07-B1-07.

7. Badea L, Herlea V, Dima SO, Dumitrascu T, Popescu I (2008) Combined gene expression analysis of whole-tissue and microdissected pancreatic ductal adenocarcinoma identifies genes specifically overexpressed in tumor epithelia. *Hepatogastroenterology* 55(88):2016–2027.

8. Balagurunathan Y, et al. (2008) Gene expression profiling-based identification of cell-surface targets for developing multimeric ligands in pancreatic cancer. *Mol Cancer Ther* 7(9):3071–3080.

9. Donahue TR, et al. (2012) Integrative survival-based molecular profiling of human pancreatic cancer. *Clin Cancer Res Off J Am Assoc Cancer Res* 18(5):1352–1363.

10. Frampton AE, et al. (2015) microRNAs with prognostic significance in pancreatic ductal adenocarcinoma: A meta-analysis. *Eur J Cancer Oxf Engl 1990* 51(11):1389–1404.

11. Grützmann R, et al. (2004) Gene expression profiling of microdissected pancreatic ductal carcinomas using high-density DNA microarrays. *Neoplasia N Y N* 6(5):611–622.

12. Iacobuzio-Donahue CA, et al. (2003) Exploration of global gene expression patterns in pancreatic adenocarcinoma using cDNA microarrays. *Am J Pathol* 162(4):1151–1162.

13. Ishikawa M, et al. (2005) Experimental trial for diagnosis of pancreatic ductal carcinoma based on gene expression profiles of pancreatic ductal cells. *Cancer Sci* 96(7):387–393.

14. Lunardi S, et al. (2014) IP-10/CXCL10 induction in human pancreatic cancer stroma influences lymphocytes recruitment and correlates with poor survival. *Oncotarget* 5(22):11064–11080.

15. Pei H, et al. (2009) FKBP51 affects cancer cell response to chemotherapy by negatively regulating Akt. *Cancer Cell* 16(3):259–266.

16. Zhang G, et al. (2012) DPEP1 inhibits tumor cell invasiveness, enhances chemosensitivity and predicts clinical outcome in pancreatic ductal adenocarcinoma. *PloS One* 7(2):e31507.

17. Subramanian A, et al. (2005) Gene set enrichment analysis: a knowledge-based approach for interpreting genome-wide expression profiles. *Proc Natl Acad Sci U S A* 102(43):15545–15550.

Supplemental Figure 1.

A.

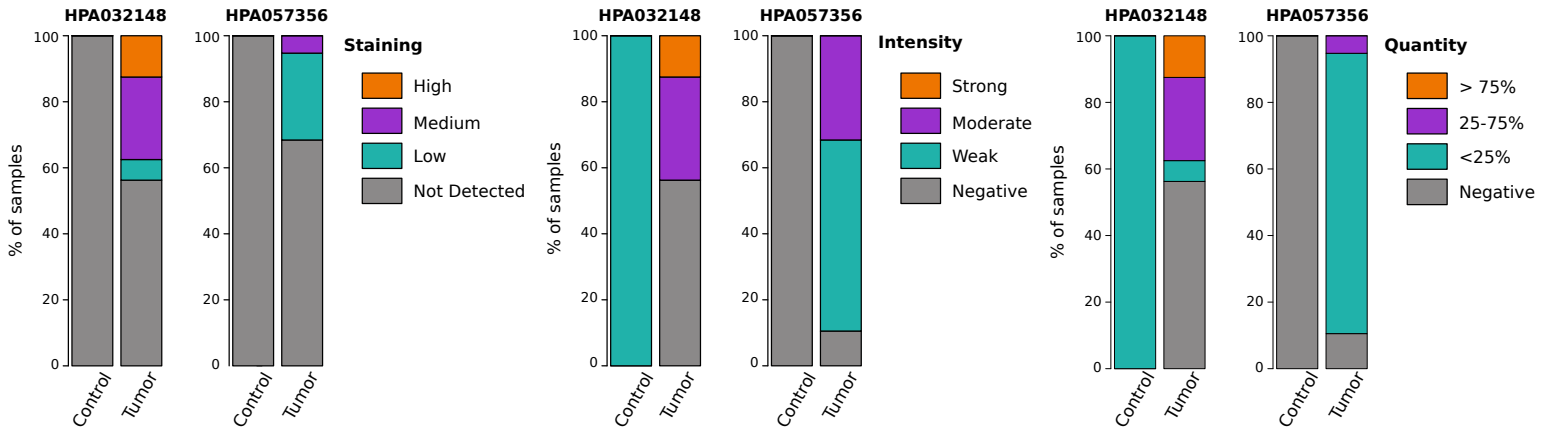

B.

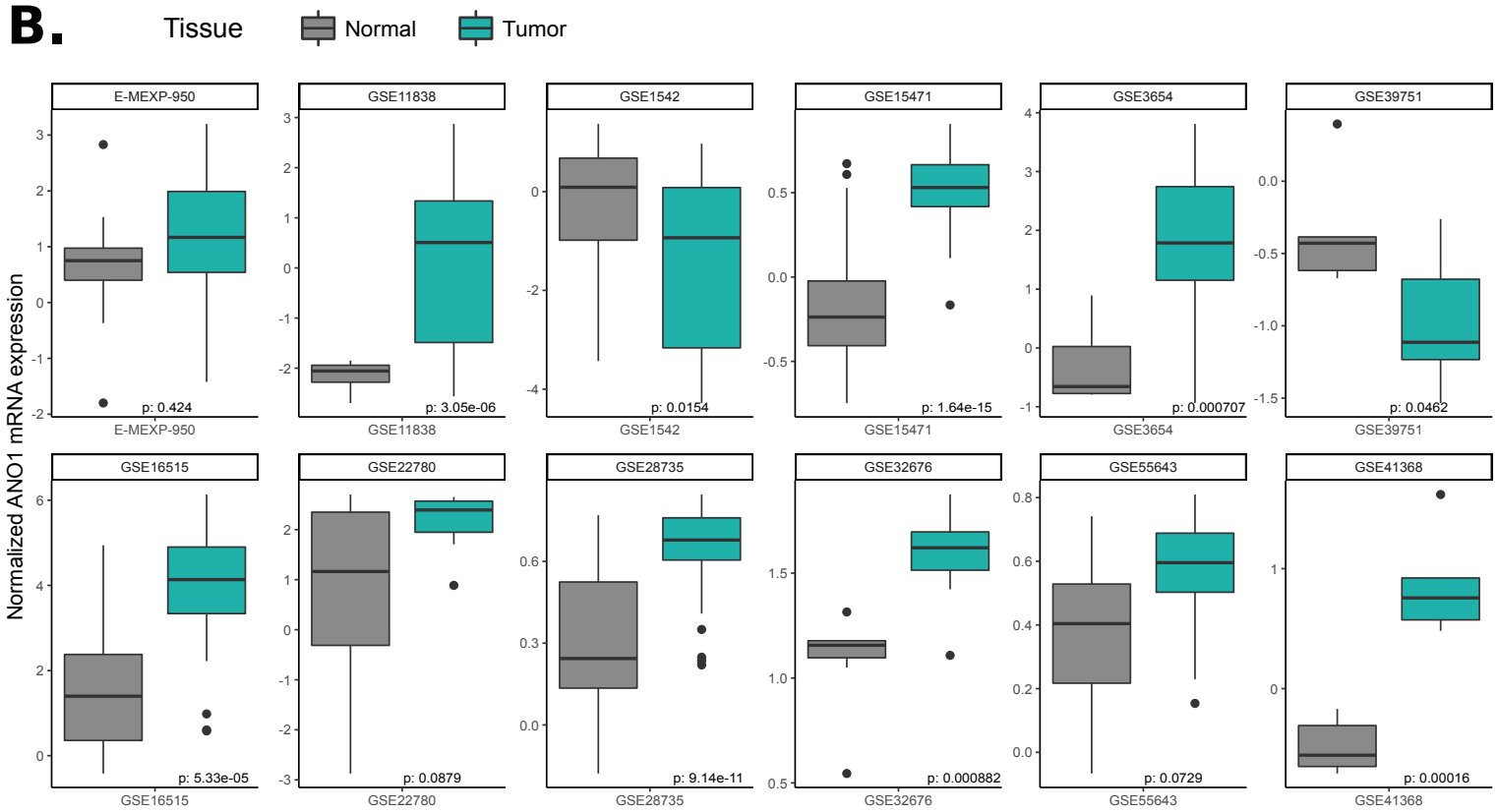

C.

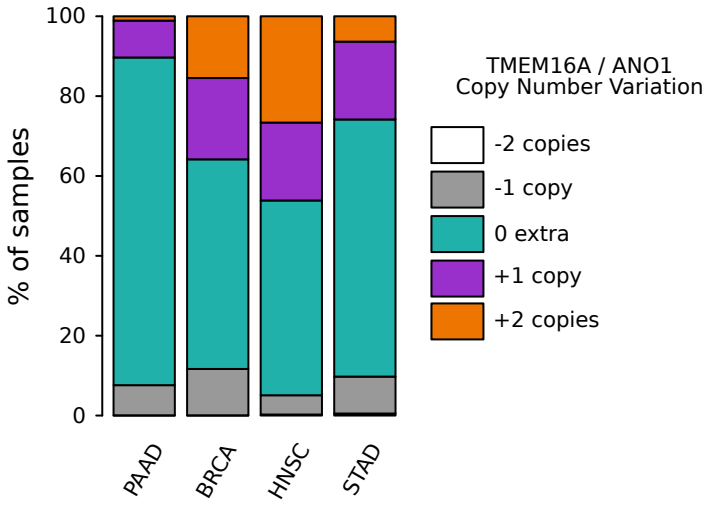

Fig. S1. TMEM16A/ANO1 mRNA is up-regulated in pancreatic cancer. (A) Images of TMEM16A immunohistochemistry stained with two different antibodies (HPA032148 and HPA057356) in normal and cancerous pancreatic tissues were obtained from Human Protein Atlas . The overall quality, intensity and quantity of the staining was evaluated. **(B)** TMEM16A/ANO1 is overexpressed in pancreatic cancers according to the signal intensities of TMEM16A mRNA expression in human normal and tumoral pancreatic cancer samples. mRNA expression values in cancerous tissues (blue boxes) are compared with corresponding normal tissues (grey boxes). **(C)** Copy number variation of TMEM16A/ANO1 gene in pancreatic cancer (PAAD), breast cancer (BRCA), head and neck squamous carcinoma (HSNC) and gastrointestinal cancer (STAD) obtaned from datasets collected by TCGA.

Supplemental Figure 2.

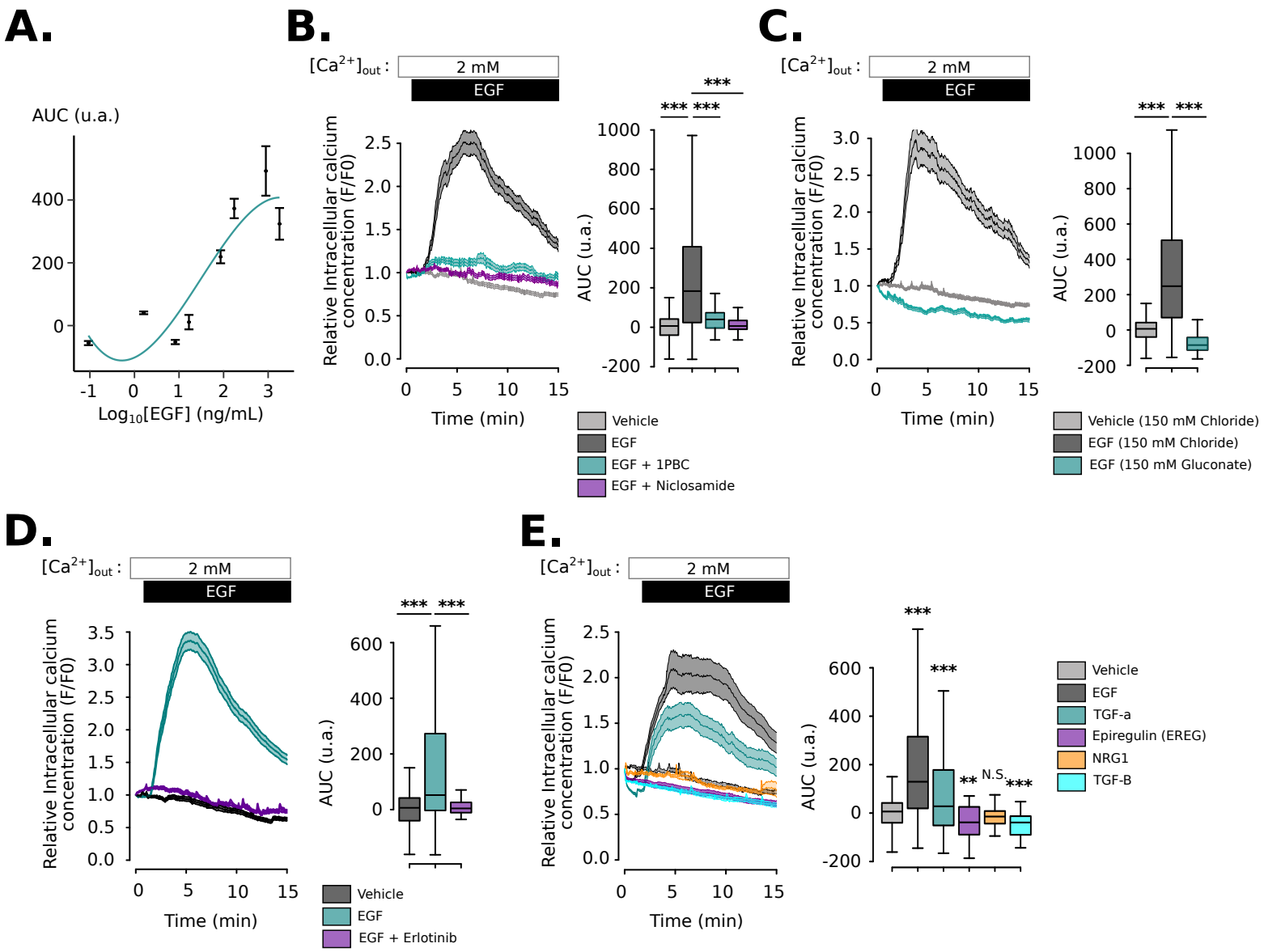

Fig. S2. Characterization of the EGF-dependent Ca^{2+} influx in AsPC-1. (A) Dose-dependent EGF-induced Ca2+ signaling. Data are mean ± SEM from 2 to 3 independent experiments regrouping 80 to 171 cells per conditions. **(B)** Relative Ca^{2+} influx (F/F_0) in AsPC-1 cells treated with EGF (50 ng/mL) alone or in combination with TMEM16A blockers 1PBC (10 µM) or Niclosamide (20 µM). Boxplots represent the corresponding integrative fluorescence signal observed from 2 independent experiments regrouping 75 to 288 cells (t-test: ***, $P < 0.001$). **(C)** Relative Ca^{2+} influx (F/F_0) in AsPC-1 cells treated with EGF (50 ng/mL) in a solution containing 150 mM Chloride or 150 mM Gluconate ions. Boxplots represent the corresponding integrative fluorescence signal observed from 2 independent experiments regrouping 155 to 198 cells (t-test: ***, $P < 0.001$). **(D)** EGF-induced Ca^{2+} signaling requires EGFR activation. Relative Ca^{2+} influx (F/F_0) in AsPC-1 stimulated with EGF (50 ng/mL) in presence or absence of Erlotinib. Histograms represent the corresponding integrative fluorescence signal observed. Data are mean ± SEM from 2 to 5 independent experiments regrouping from 50 to 162 cells per condition (t-test: ***, $P < 0.001$). **(E)** Only TGF-α and EGF induces Ca^{2+} influx in AsPC-1. Relative Ca^{2+} (F/F_0) in AsPC-1 stimulated with various growth factors (EGF, TGF-α, EREG (Epiregulin), NRG-1 (Neuregulin-1), TGF-β1 (Tranforming Growth Fator Beta-1)). Histograms represent the corresponding integrative fluorescence signal observed. Data are mean ± SEM from 2 to 4 independent experiments regrouping 80 to 198 cells per condition (t-test: ***, $P < 0.001$).

Supplemental Figure 3.

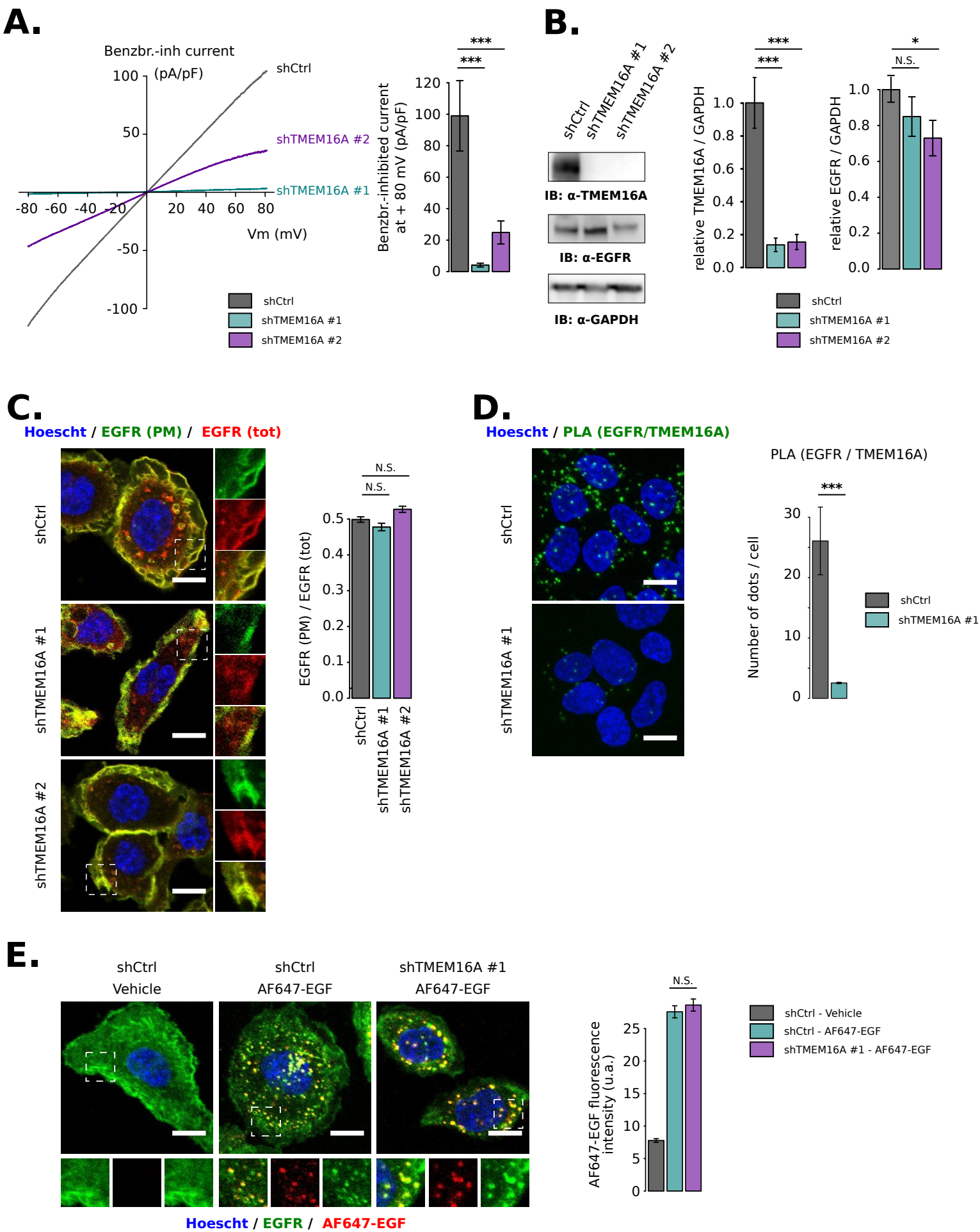

Fig. S3. Validation of shRNA knockdown of TMEM16A in AsPC-1 and its impact on EGFR expression and EGF endocytosis. (A) Validation of TMEM16A silencing by shRNA in AsPC-1. Representative benzbromarone-inhibited chloride currents recorded from voltage ramps from -80 to +80 mV in whole cell patch-clamp of control (shCtrl) and TMEM16A-silenced (shTMEM16A #1, shTMEM16A #2) AsPC-1 cells. Right, histograms represent the corresponding current amplitude. Values are mean ± SEM (8 to 10 cells; Mann-Whitney: * $P < 0.05$). **(B)** Left, representative western blots showing the TMEM16A extinction and EGFR expression in shTMEM16A AsPC-1 cells (shTMEM16A #1, shTMEM16A #2) when compared to control cells (shCtrl). Right, corresponding histograms representing TMEM16A and EGFR expression normalized with GAPDH expression. Data are mean ± SEM from 11 to 14 independent experiments (Mann-Whitney: ***, $P < 0.001$, *, $p < 0.05$, N.S., $p > 0.05$). **(C)** Representative images from confocal microscopy showing the distribution of EGFR at the plasma membrane (PM) (in green) and in the entire cell (in red). Right, corresponding histograms showing the ratio of the relative fluorescence signal measured at the PM over the relative fluorescence signal observed in the entire cell. Data are mean ± SEM from 2 independent experiments regrouping 18 to 42 cells per condition (Mann-Whitney: *, $P < 0.05$). **(D)** *in situ* proximity ligation assay (PLA) quantifying the number of complexes between TMEM16A and EGFR in control (shCtrl) and TMEM16A-silenced (shTMEM16A #1) AsPC-1 cells. Left, representative images showing protein interaction areas (yellow dots) and cell nuclei stained with Hoescht 33342 (blue). Right, corresponding quantification of dot/cell density. Results are representative of three independent experiments. 10 fields per condition were analyzed in each experiment (Mann-Whitney: ***, $P < 0.001$;. N.S., non-significant). E. EGF endocytosis was evaluated after an acute application of AlexaFluor647-conjugated EGF (100 ng/mL) for 15 min at 37°C. Left, representative images from confocal microscopy showing internalized AlexaFluor647-conjugated EGF (Red) and endogenous EGFR (green) in control (shCtrl) and TMEM16A-silenced (shTMEM16A#1) AsPC-1 cells. Right, corresponding histograms representing the AlexaFluor647-conjugated EGF fluorescence intensity measured in each conditions. Data are mean ± SEM from 2 independent experiments representing 30 to 50 cells (t-test: N.S., Non-Significant).

Supplemental Figure 4.

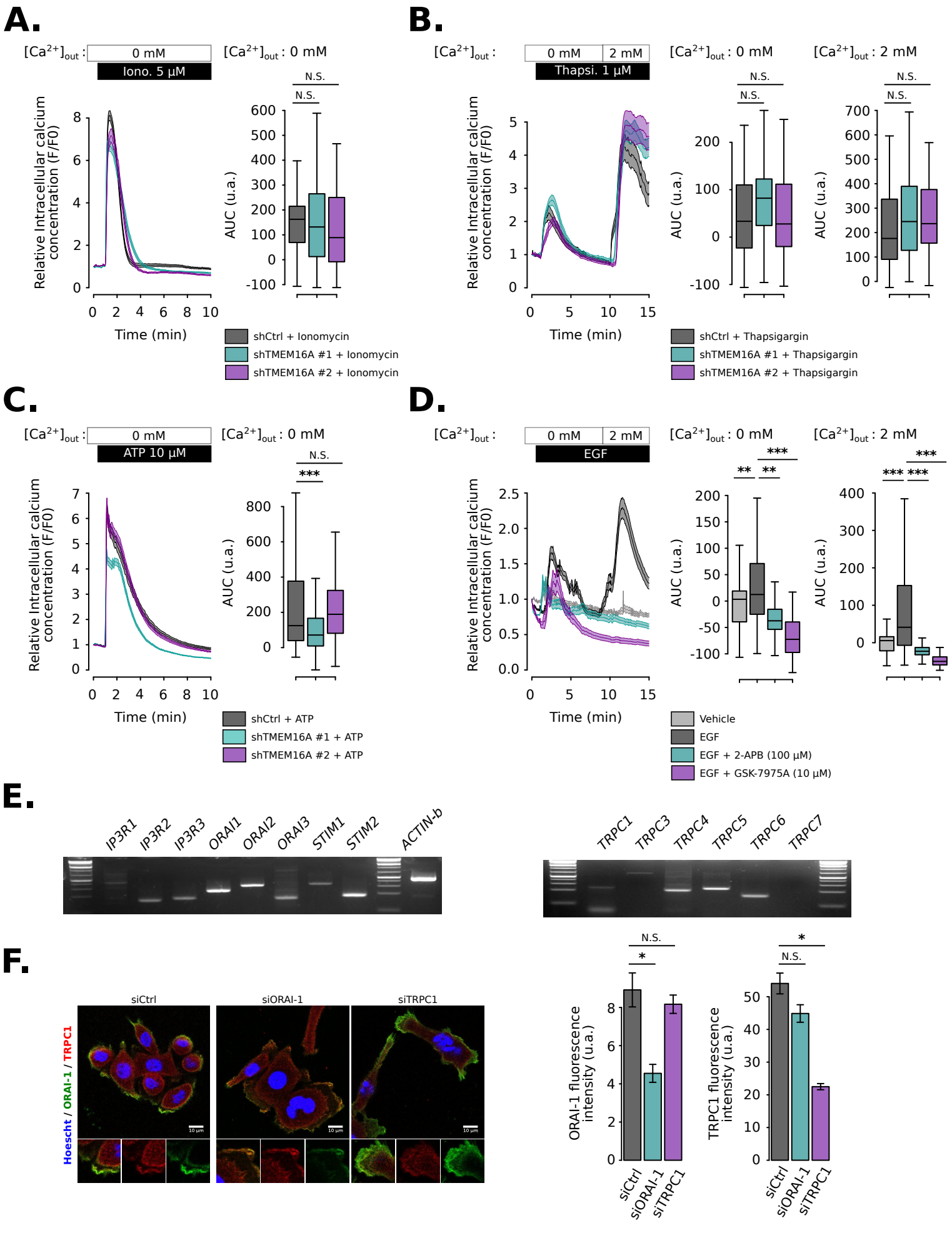

Fig. S4. Contribution of TMEM16A to intracellular store Ca^{2+} content, IP_3-independent or P2YR-induced IP_3-dependent Store-Operated Ca^{2+} Entry and identification of Store-Operated Ca^{2+} Channels expressed in AsPC-1 and validation of siRNA silencing for ORAI-1 and TRPC-1. (A) Relative Ca^{2+} influx (F/F_0) in control (shCtrl) and TMEM16A-silenced (shTMEM16A #1, shTMEM16A #2) AsPC-1 cells treated with Ionomycin (5 µM) in a Ca^{2+}-free buffer for 10 min. Boxplots represent the corresponding integrative fluorescence signal observed from 2 independent experiments regrouping 108 to 153 cells per condition (t-test: ***, $P < 0.001$). **(B)** Relative Ca^{2+} influx (F/F_0) in control (shCtrl) and TMEM16A-silenced (shTMEM16A #1, shTMEM16A #2) AsPC-1 cells treated with Thapsigargin (Tg) (1 µM) in a Ca^{2+}-free buffer for 10 min and a 2 mM Ca^{2+} buffer for 5 min. Boxplots represent the corresponding integrative fluorescence signal observed from 2 independent experiments regrouping 62 to 65 cells per condition (t-test: ***, $P < 0.001$). **(C)** Relative Ca^{2+} influx (F/F_0) in control (shCtrl) and TMEM16A-silenced (shTMEM16A #1, shTMEM16A #2) AsPC-1 cells treated with ATP (10 µM) in a Ca^{2+}-free buffer for 10 min. Boxplots represent the corresponding integrative fluorescence signal observed from 3 independent experiments regrouping 188 to 287 cells per condition (t-test: ***, $P < 0.001$). **(D)** Relative Ca^{2+} influx (F/F_0) in AsPC-1 cells treated with EGF (50 ng/mL) alone or in combination with SOCE inhibitor, 2-APB (100 µM) or ORAI1 inhibitor GSK-7975A (10 µM) in a Ca^{2+}-free buffer for 10 min and a 2 mM Ca^{2+} buffer for 5 min. Boxplots represent the corresponding integrative fluorescence signal observed from 2 to 4 independent experiments regrouping 81 to 195 cells per condition (t-test: ***, $P < 0.001$). **(E)** RT-PCR demonstrates mRNA expression of Store-Operated Ca^{2+} channels (ORAI and TRPC channel families) and intracellular Ca^{2+} channels (IP_3R family) and intracellular Ca^{2+} sensor (STIM1 and STIM2) in AsPC-1 cells. **(F)** Representative images showing the subcellular distribution of ORAI-1 (in green) and TRPC-1 (in red) by immunofluorescent staining in control (siCtrl) or AsPC-1 silenced for ORAI-1 (siORAI1) or TRPC-1 (siTRPC1). Histograms represent the relative fluorescence intensity measured in individual cells. Data are mean ± SEM from 2 independent experiments regrouping 10 to 13 cells per condition (Mann-Whitney: *, $P < 0.05$).

Supplemental Figure 5.

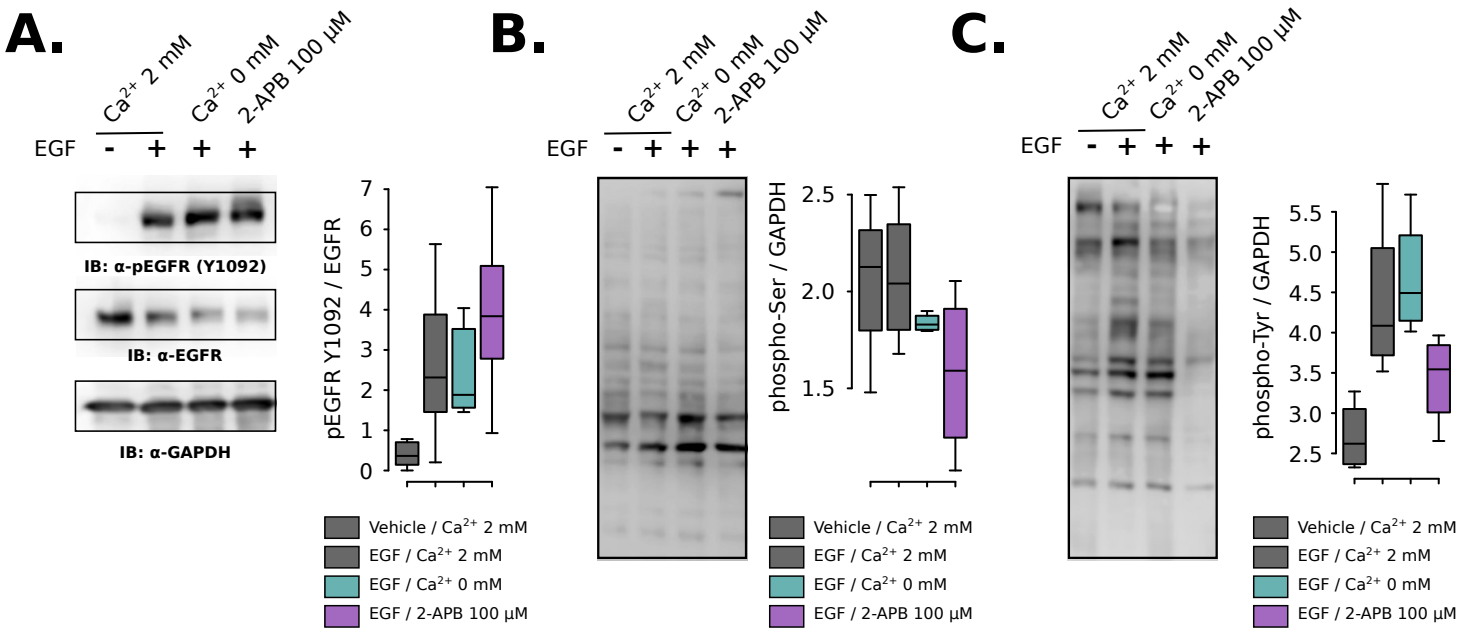

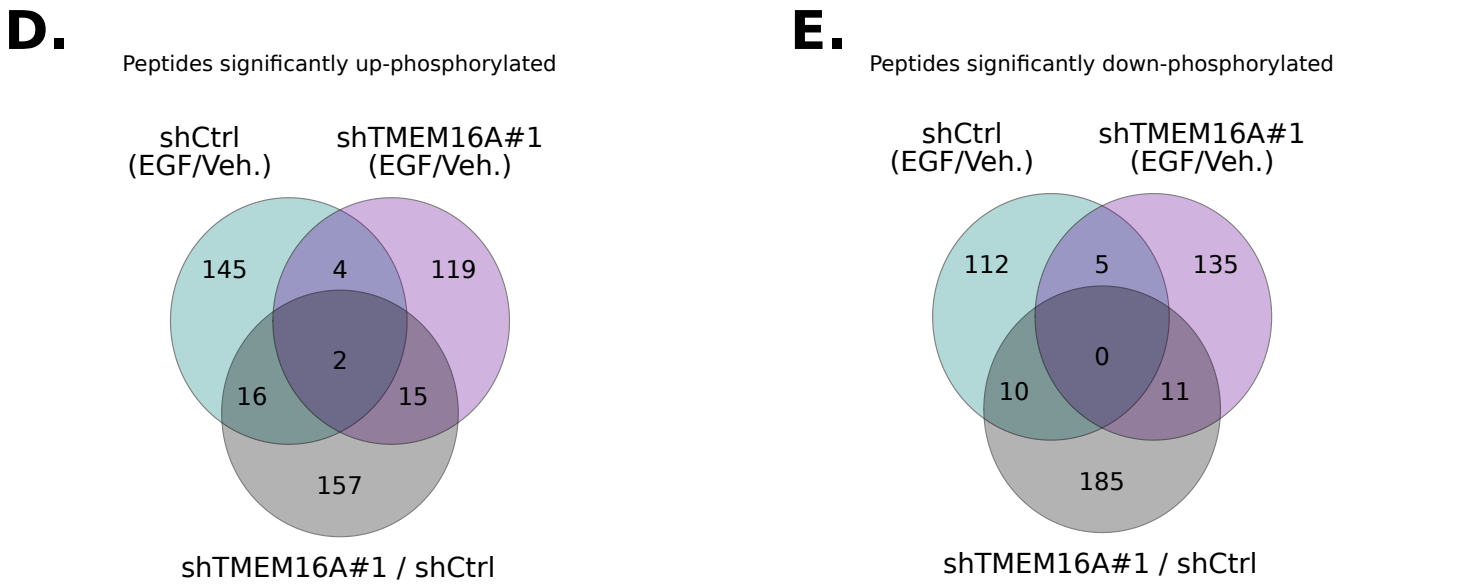

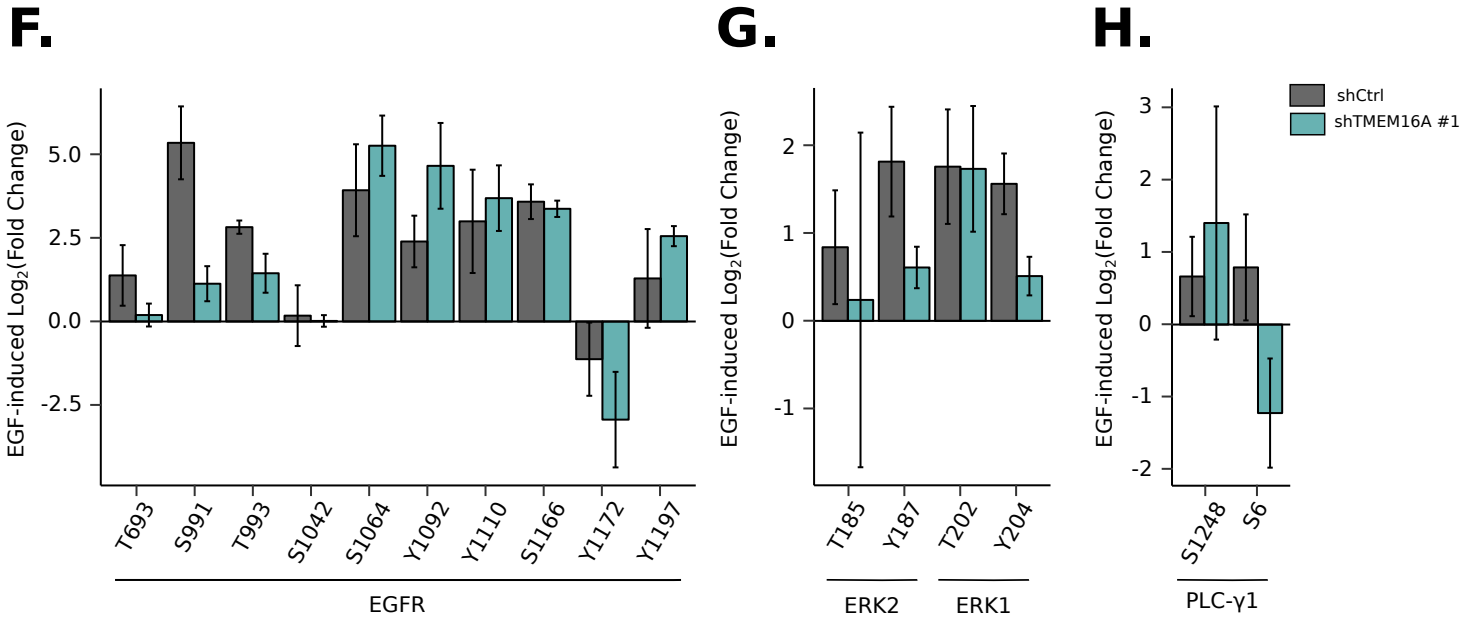

Fig. S5. TMEM16A silencing partially reproduces EGF-induced remodeling of phosphoproteome in AsPC-1. Total protein extracts from AsPC-1 cells treated or not with EGF (50 ng/mL) for 30 min alone or in combination of SOCE inhibitor 2-APB (100 µM) or in a Ca2+-free buffer (Ca2+ 0 mM) were separated on SDS-PAGE and immunoblotted with different antibodies. **(A)** Representative western blot obtained with anti-phosphorylated EGFR (Y1092), and anti-EGFR antibodies. Right, corresponding boxplots representing the ratio of phosphorylated over total EGFR normalized with GAPDH expression. **(B)** Representative western blot obtained with anti-phosphorylated Serine. Right, corresponding boxplots representing the total phosphorylated Serine normalized with GAPDH expression from 4 independent experiments. **(C)** Representative western blot obtained with anti-phosphorylated Tyrosine. Right, corresponding boxplots representing the total phosphorylated Tyrosine normalized with GAPDH expression from 4 independent experiments. Phosphoproteome of control (shCtrl) and TMEM16A-silenced (shTMEM16A #1) AsPC-1 cells treated in the presence or absence of EGF (50ng/mL) for 30 min was determined. Log_2 values for each peptides were calculated from data obtained in 3 independent experiments. For each peptides, log_2(Fold Change) and corresponding p values were calculated when comparing 1) control cells treated by EGF with control cells treated by vehicle (shCtrl+EGF/shCtrl), 2) TMEM16A-deficient cells treated with EGF and TMEM16A-deficient cells treated with vehicle (shTMEM16A+EGF/shTMEM16A) and when comparing 3) TMEM16A-deficient cells and control cells (shTMEM16A/shCtrl). **(D)** Venn diagramm representing the overlap of significantly up-phosphorylated peptides in shCtrl+EGF/shCtrl, shTMEM16A+EGF/shTMEM16A and shTMEM16A/shCtrl. **(E)** Venn diagramm representing the overlap of significantly down-phosphorylated peptides in shCtrl+EGF/shCtrl, shTMEM16A+EGF/shTMEM16A and shTMEM16A/shCtrl. **(F)** Histograms representing the EGF-induced log_2(Fold Change) for individual phosphorylated sites of EGFR detected in control (shCtrl) and TMEM16A-silenced (shTMEM16A#1) AsPC-1 cells. **(G)** Histograms representing the EGF-induced log_2(Fold Change) for individual phosphorylated sites of ERK1/2 detected in control (shCtrl) and TMEM16A-silenced (shTMEM16A#1) AsPC-1 cells. **(H)** Histograms representing the EGF-induced log_2(Fold Change) for individual phosphorylated sites of PLC-γ1 detected in control (shCtrl) and TMEM16A-silenced (shTMEM16A#1) AsPC-1 cells.

Dataset S1: Results from differential expression analysis (DEA) and Gene Set Enrichment Assay (GSEA) between “High TMEM16A” and “Low TMEM16A” pancreatic tumors.

Dataset S2: List of phosphorylated peptides detected in control and TMEM16A-deficient AsPC-1 cell lines in the presence or absence of EGF stimulation and calculation of EGF-induced fold change (log_2(FC)) and the corresponding p-value of the phosphorylation level of each of these residues in control and TMEM16A-silenced cells.

Dataset S3: Clinical data associated with different clusters obtained in Figure 6.

Dataset S4: List of reagents and primers used